The IFS dynamical core and its new features in openIFS cycle 48r1

Michail Diamantakis

A hands-on introduction to Numerical Weather Prediction Models

15 November 2023

ECMWF

Talk Outline

- Equation sets, grids, and dynamical core overview
- Motivation, historical context for the introduction of semi-implicit, semi-Lagrangian methods
- Fundamental algorithms and their limitations
- The pros and cons of the IFS formulation:
  - conservation aspects and errors in IFS and how we deal with them
- Atlas, Atlas multiple grids and applications on advection

The ECMWF hydrostatic global operational model equation set

$$\frac{D\mathbf{V}_h}{Dt} + f\mathbf{k}\times\mathbf{V}_h + \nabla_h\Phi + R_d T_v \nabla_h \ln p = P_{\mathrm{v}}$$

$$\frac{DT}{Dt} - \frac{\kappa T_v \omega}{(1+(\delta-1)q)\,p} = P_{\mathrm{T}}$$

$$\frac{Dq_x}{Dt} = P_{\mathrm{q}_x}$$

$$\frac{\partial}{\partial t}\left(\frac{\partial p}{\partial\eta}\right) + \nabla_h\cdot\left(\mathbf{V}_h\frac{\partial p}{\partial\eta}\right) + \frac{\partial}{\partial\eta}\left(\dot{\eta}\frac{\partial p}{\partial\eta}\right) = 0$$

$$\Phi = \Phi_s - \int_1^{\eta} R_d T_v \frac{\partial}{\partial\eta}(\ln p)\,d\eta$$

η : hybrid pressure based vertical coordinate
$\mathbf{V}_h$: horizontal wind components u, v
T: temperature
T_v: virtual temperature (used as spectral variable)
q_x: specific humidity, specific ratios for cloud fields and other tracers x, $\delta=c_{pv}/c_{pd}$
Φ: geopotential
p : pressure
ω=dp/dt : diagnostic vertical velocity
P: physics forcing terms

- Primitive equation hydrostatic (non-hydrostatic version available but not operational)
- Spectral Transform method in the horizontal on spherical harmonics basis functions
- Cubic spline Finite Elements in the vertical
- Time-stepping: semi-Lagrangian semi-implicit

} Space-discretization

Solving the equations: spectral transform Semi-implicit semi-Langrangian (SISL) method

Grid-point calculations
-semi-Lagrangian advection
-physical parametrizations
-products of terms

FFT

Fourier space

LT

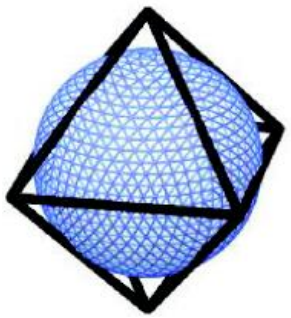

Spectral calculations
-horizontal gradients
-semi-implicit correction
-horizontal diffusion

Inverse LT

Fourier space

Inverse FFT

FFT: Fast Fourier Transform, LT: Legendre Transform

<u>Vertical discretization</u>

- Hybrid pressure based vertical coordinate $\eta(p)$
- 8^{th} order Finite Element discretization based on cubic basis functions
  - Accurate vertical integrals with benefits seen mostly in the stratosphere
  - More accurate vertical velocity

Cycle 48r1 scheme upgrade based on work by Vivoda et al, 10.1175/MWR-D-18-0043.1:

- Unified for hydrostatic and non-hydrostatic
- Better for single precision(SP) – IFS runs SP forecasts from cycle 47r2

ECMWF

Spectral transforms on spherical harmonics

Spherical harmonics

Spectral coefficient longitude latitude

$$f(\lambda,\phi) = \sum_{m=-\infty}^{\infty} \sum_{n=|m|}^{\infty} f_n^m Y_n^m(\lambda,\phi), \quad Y_n^m(\lambda,\phi) = P_n^m(\sin\phi)\, e^{im\lambda}$$

m: zonal wavenumber
n: total wavenumber

Associated Legendre Polynomials (normalised)

- **We can compute derivatives without approximations using analytical formulae**
- **The common “pole singularity” problem is overcome**
- **Spherical harmonics are the eigenfunctions of the Laplace operator: in time-stepping the derived “Helmholtz equation” can be decoupled and solved by a very cheap & simple diagonal solver**

- **Advancements in algorithms, hardware and software have enabled us to keep running efficiently the spectral transform method at ever increasing resolutions**
- **ecTrans: a multi-node GPU enabled spectral transform library (Hybrid24 project)**

Improved accuracy, efficiency and scalability with octahedral reduced cubic A-grid (41r2 and later cycles)

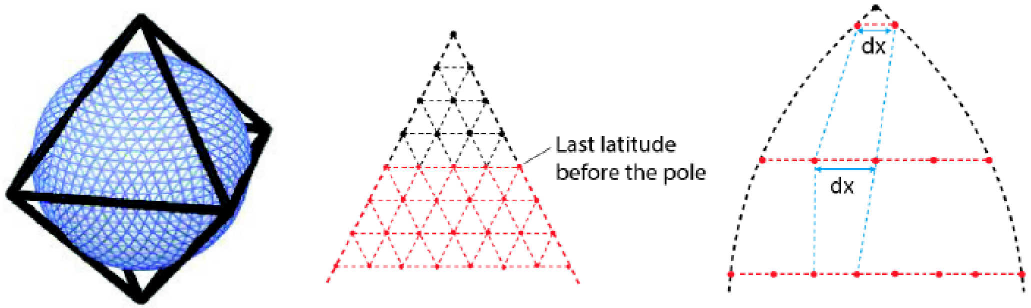

Collignon projection on the sphere: $Nlati = 4 \times i + 16,\ \ i = 1, \ldots, N$

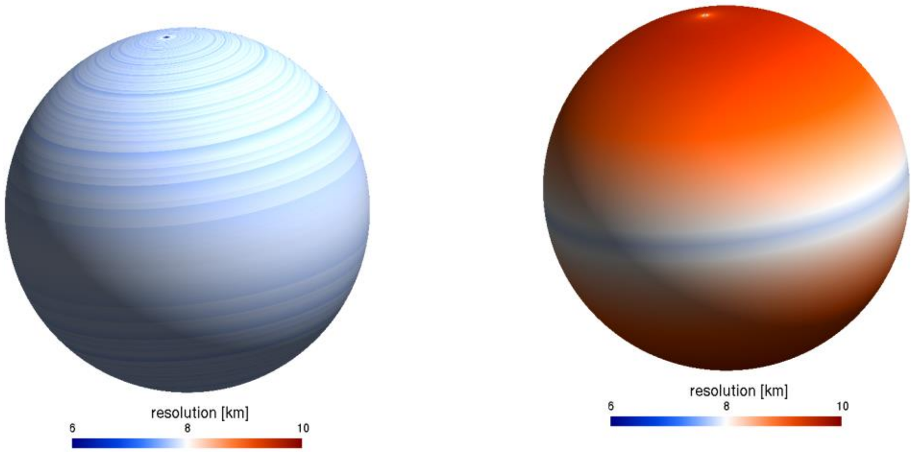

Latitudinal variation of resolution for standard cubic grid and octahedral cubic grid

Reference: "A new grid for the IFS" ECMWF newsletter 146, Winter 2015-2016, Malardel et al

Benefits of cubic octahedral grid compared with old linear grid:

- Improved effective resolution
- Improved total mass conservation
- Improved efficiency and scalability (higher gridpoint resolution, same spectral truncation)

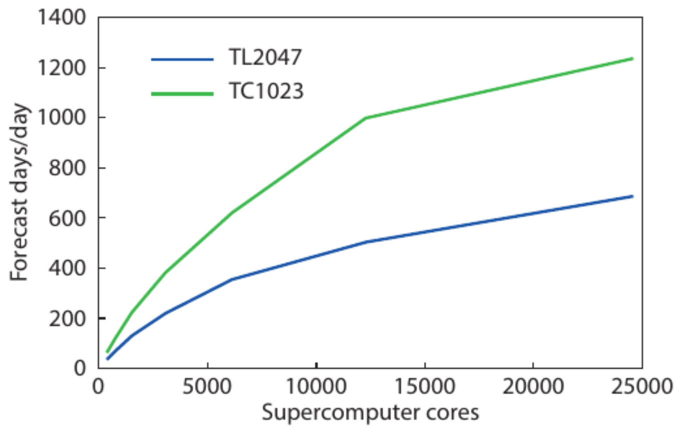

Above: cubic versus linear grid run at same gridpoint resolution. Plotted: forecast days / day per number of cores. Note that at high number of cores the rate achieved with a cubic grid is twice as large as the one by the linear!

Virtues of semi-implicit semi-Lagrangian techniques

Semi-Lagrangian (SL) semi-implicit (SI) technique is ideal for global NWP – stable, efficient and accurate integration of the governing equations

- ❑ Unconditionally stable SL advection scheme with small phase speed errors and little numerical dispersion
  - ✓ No CFL restriction in timestep: large timesteps can be used without accuracy penalty ☺
  - ✓ Multi-tracer efficient
- ❑ Unconditionally stable SI time stepping for the integration of other dynamical processes than advection
  - ✓ No timestep restriction from the integration of “fast forcing” terms such as gravity wave and acoustic terms (exclusively in non-hydrostatic models)
  - ✓ 2^{nd} order accuracy

History of semi-Lagrangian method at ECMWF

- Until the beginning of 1991 IFS was a spectral semi-implicit Eulerian model on a full Gaussian grid at T106 horizontal resolution and 19 levels
  - An increase to T231 L31 resolution was planned
  - This upgrade required at least 12 x available CPU power
  - Funding was available for 4 x CPU increase …
- Upgrade was made possible only due to switching to:
  - A semi-Lagrangian scheme on a reduced Gaussian grid
  - The new model was 6 x faster!

Semi-Lagrangian advection in a picture

SL is a numerical technique for solving advection type PDEs which applies *Lagrangian* type of calculations on grid-point models

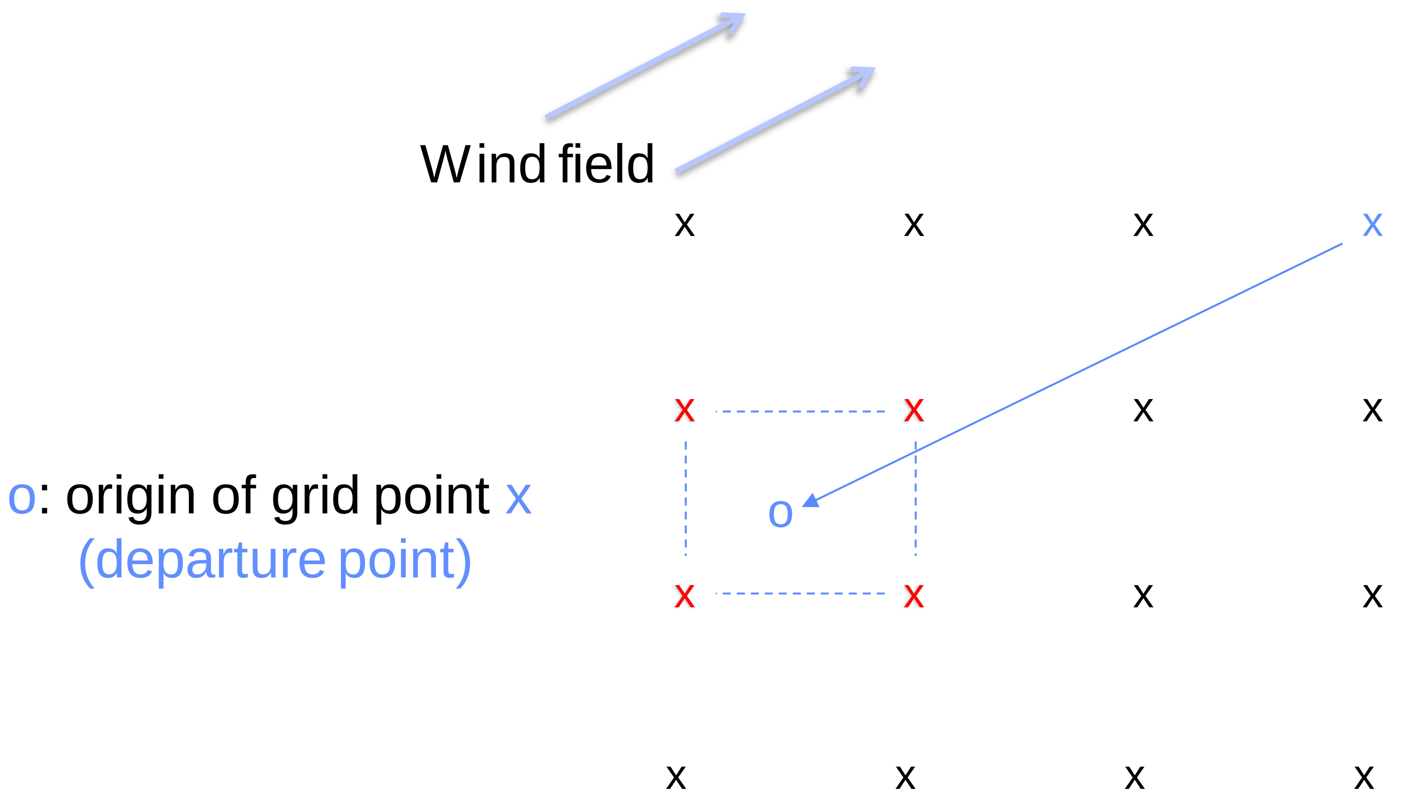

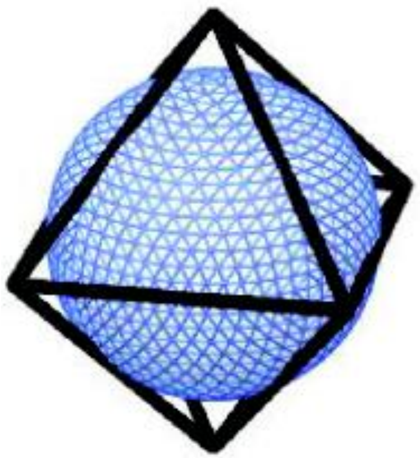

The SL solution of the advection equation

Start with the simple passive tracer advection equation (constant wind):

$$\frac{D\phi}{Dt} \equiv \frac{\partial \phi}{\partial t} + V \cdot \nabla \phi = 0, \qquad V = (u, v, w)$$

At time t parcel is at d and at t +Δt arrives at a grid-point

$$\int_{(r_d, t)}^{(r_a, t+\Delta t)} \frac{D\varphi}{Dt} Dt = 0 \Rightarrow \varphi_a^{t+\Delta t} = \varphi_d^t, \quad r = (x, y, z)$$

This is the known result: $\varphi(r, t+\Delta t) = \varphi(r - \Delta t V, t)$

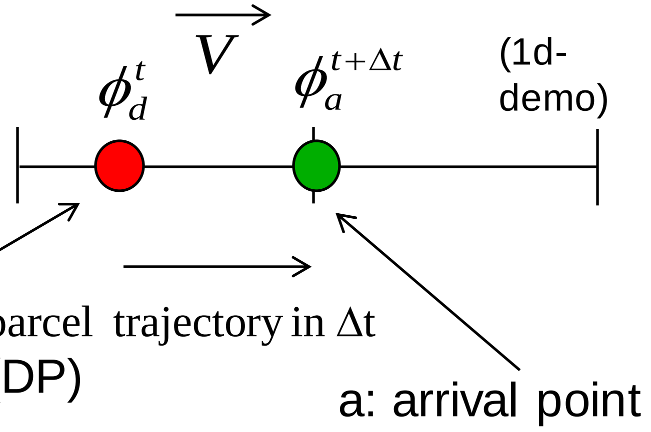

d: **departure point** (DP)

- Solution at t+Δt is obtained by finding the DP location and interpolating the available (defined at time t) grid-point ϕ values at the DP
- Eulerian advection term $V \cdot \nabla \phi$ is not explicitly computed – it is absorbed by the Lagrangian derivative (advection problem is reduced to interpolation)

Computing the departure points in real atmospheric flows: SETTLS

Consider that air parcels move in time in straight line trajectories. Perform a 2nd order Taylor expansion of an arrival (grid) point to its departure point:

Stable Extrapolation Two Time Level Scheme (Hortal, QJRMS 2002)

$$r_a(t+\Delta t) = r_d(t) + \Delta t \cdot \left(\frac{Dr}{Dt}\right)_d^t + \frac{\Delta t^2}{2} \cdot \left(\frac{D^2 r}{Dt^2}\right)_{AV}$$

AV: average value along SL trajectory

$$\left(\frac{Dr}{Dt}\right)_d^t = V_d(t), \qquad \left(\frac{D^2 r}{Dt^2}\right)_{AV} = \left(\frac{DV}{Dt}\right)_{AV} \approx \frac{V_a(t) - V_d(t-\Delta t)}{\Delta t}$$

Hence,

$$r_a(t+\Delta t) \approx r_d(t) + \frac{\Delta t}{2} \cdot \left(V_a(t) + \{2V(t) - V(t-\Delta t)\}_d\right)$$

DP can be computed by iterative sequence based on above SETTLS formula :

$$r_d^{(k)} = r_a - \frac{\Delta t}{2} \cdot \left(V_a(t) + \{2V(t) - V(t-\Delta t)\}\Big|_{r_d^{(k-1)}}\right) \quad k = 1, 2, \ldots K$$

Until cycle 47r3: K=4, $r_d^{(0)}$ =initial guess

Interpolate at $r_d^{(k-1)}$

Departure point iterations convergence

- SETTLS scheme for computing the departure point is iterative
- Its convergence depends on Lipschitz number magnitude. Let $\mathbf{r_D}^{[\nu]}$ an estimate of the departure point D at iteration number *v.* Then:

$$\|\mathbf{r_D}^{[\nu]} - \mathbf{r_D}^{[\nu-1]}\| \leq L\|\mathbf{r_D}^{[\nu-1]} - \mathbf{r_D}^{[\nu-2]}\|, \quad \nu = 2, 3 \ldots, \nu_{max}$$

$$L \equiv \Delta t \|\frac{\partial \mathbf{V}}{\partial \mathbf{r}}\| \qquad \text{Lipschitz (deformational Courant) number}$$

- $L < 1$ is a sufficient condition for convergence
- L is an upper bound of the rate of convergence

What happens in IFS?

Reference: Diamantakis & Magnusson MWR2016 doi:10.1175/MWR-D-15-0432.1

Lipschitz numbers in IFS forecasts

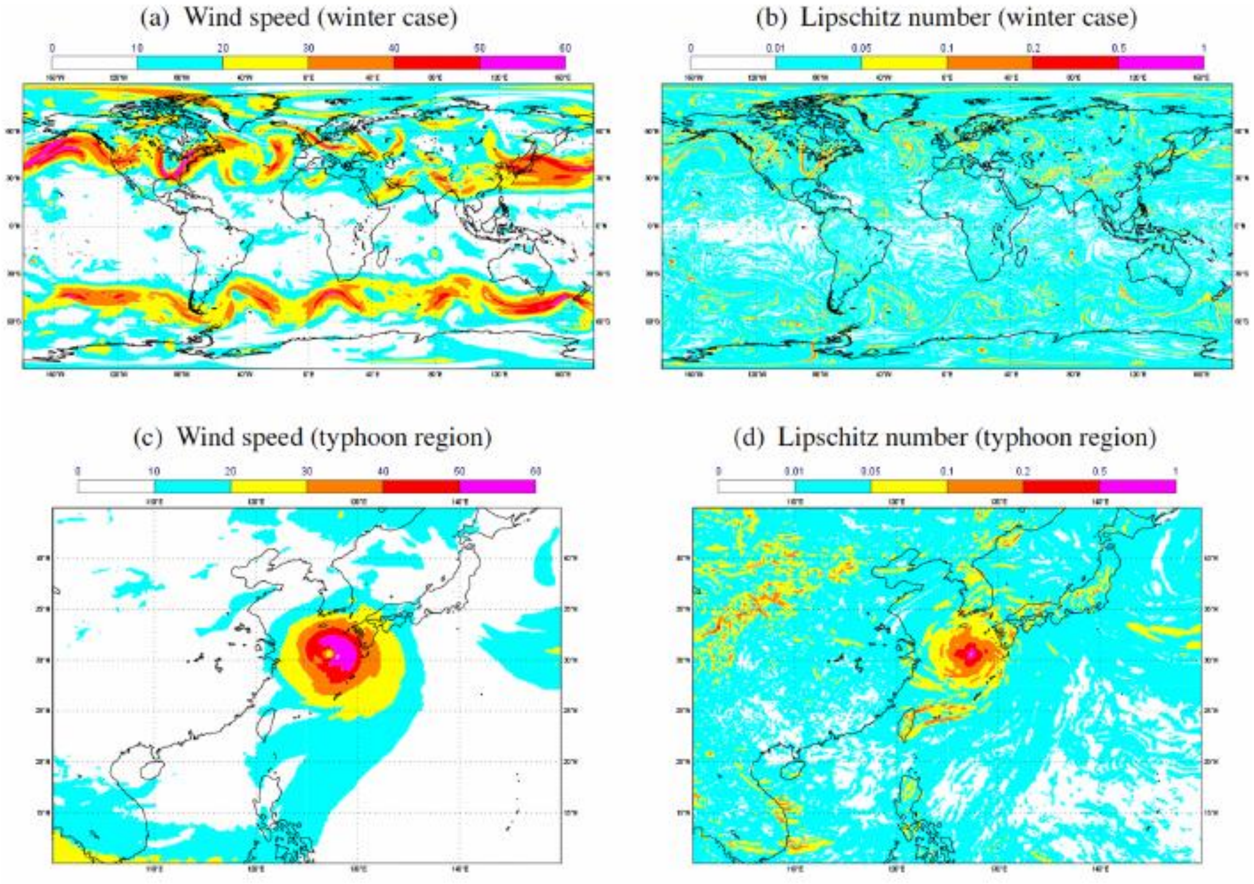

(a), (b): 00UTC 10 January 2014, t+48hrs fc at 500hPa. (c), (d): 00UTC 5 July 2014 t+96 hrs fc at 850hPa

DP convergence in typhoon Neoguri

Plots from a model level near 850 hPa: DP vertical distance between two successive iterations scaled by grid length

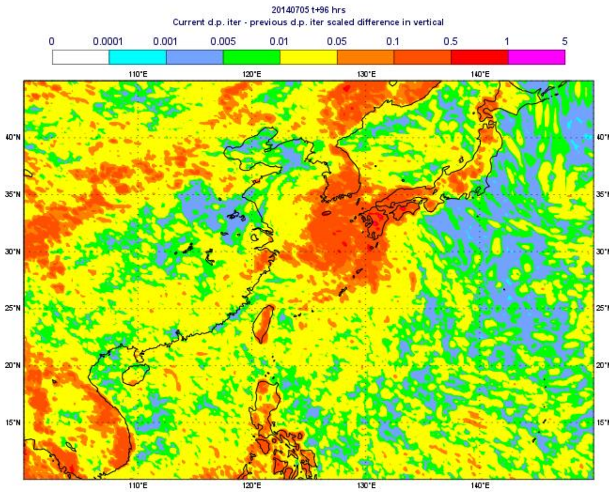

iter1–iter0

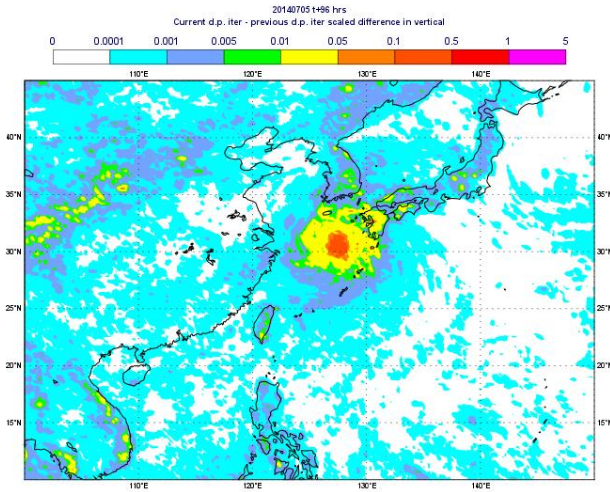

iter2–iter1

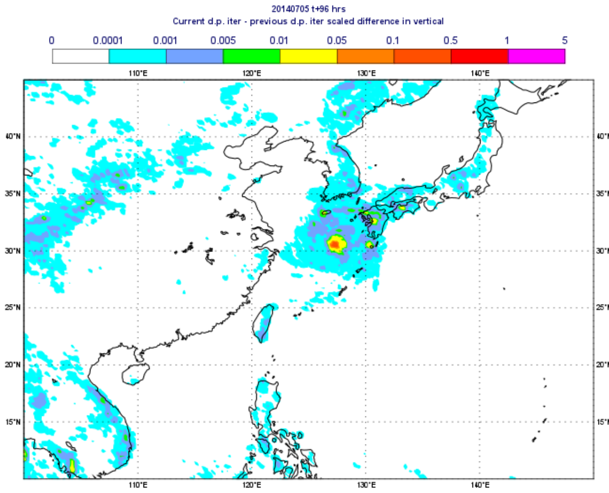

iter3–iter2

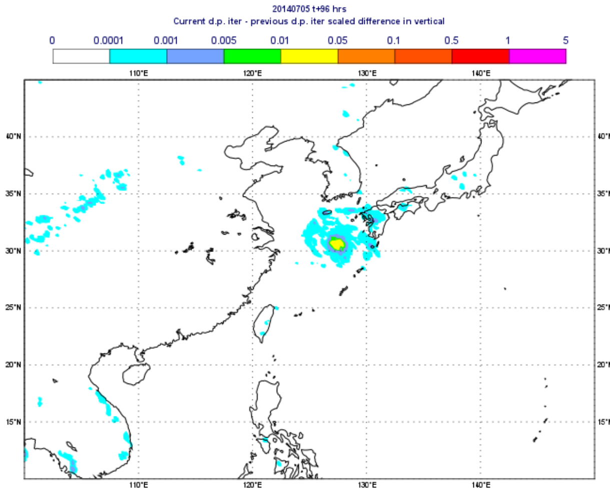

iter4–iter3

Side-effects of non-converging DP iterations

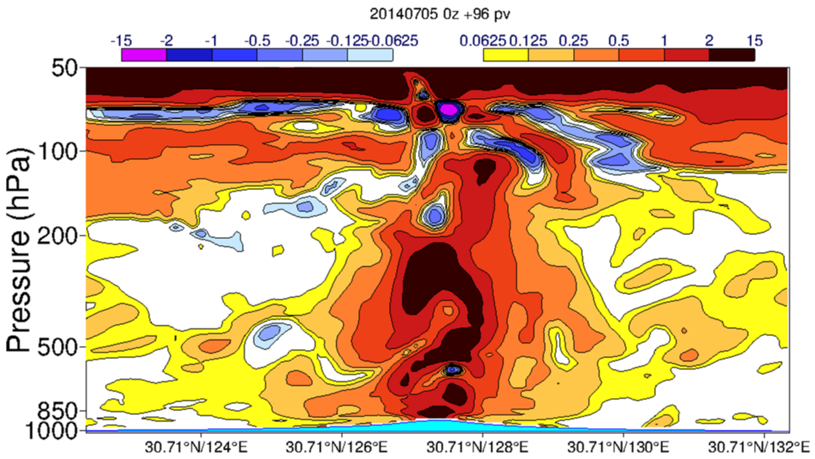

DP iterations haven’t converged

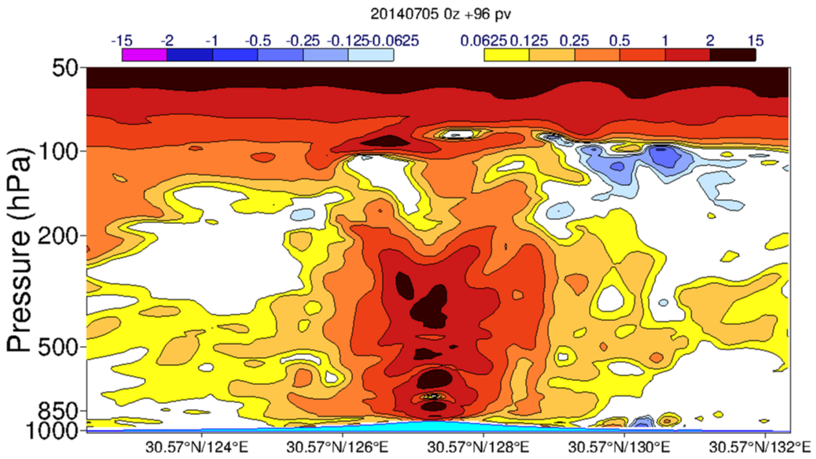

DP converged with additional iterations

- Before cy48r1: 5 DP iterations needed for sufficient convergence
- Cycle 48r1: fast convergence in 3 iterations starting from previous timestep DPs (Diamantakis & Vana, QJRMS 2021)

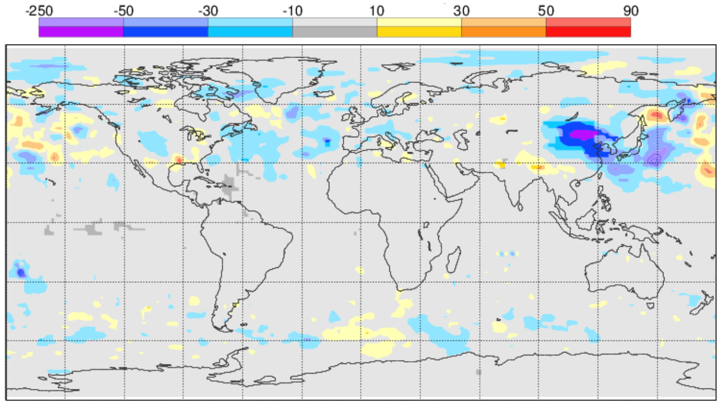

Root Mean Square Error difference for the geopotential height when DP iterations have not sufficiently converged

Computing Semi-Lagrangian departure points on the sphere in cycle 48r1

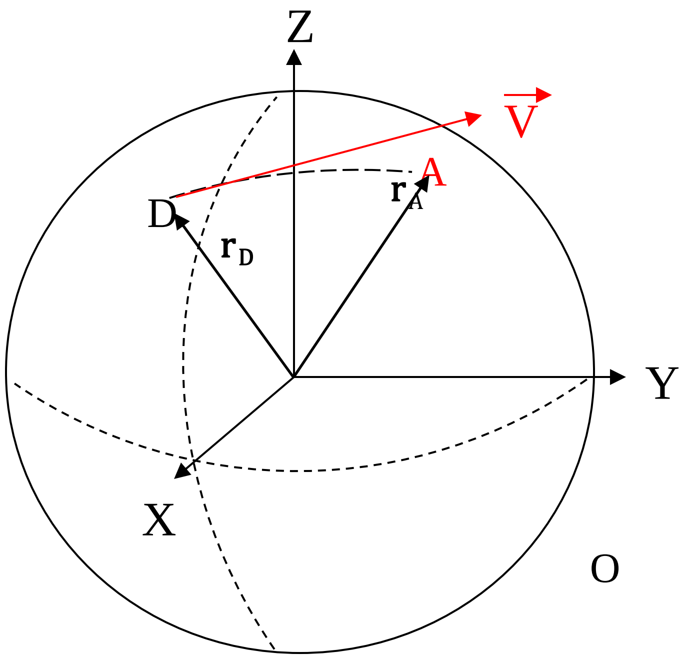

In cycle 48r1 SL departure point (**DP**) calculation on the sphere has been *simplified, improved for single precision and made more efficient* (Diamantakis & Vana QJRMS 2021 10.1002/qj.4224). The new scheme performs computations in a Cartesian framework

1. Horizontal velocities (u,v) are (linearly) transformed in a geocentric Cartesian system (X, Y, Z)
2. Apply SETTLS iterative scheme in 4D to compute $r_d = (X_d, Y_d, Z_d, \eta_d)$, η_d: transformed vertical coordinate
3. SETTLS iterations are starting using computed DP values from previous timestep which gives faster convergence, saves 2 iterations ☺
4. At each SETTLS iteration, lon/lat of DP (λ_d, θ_d) is found from

$$(X_d, Y_d, Z_d) \longrightarrow \begin{array}{l} \lambda_d = ATAN2(Y_d, X_d) \\ \theta_d = \arcsin \dfrac{Z_d}{\sqrt{X_d^2 + Y_d^2 + Z_d^2}} \end{array}$$

Special treatment for stratospheric warming predictions

- In "Sudden Stratospheric Warmings" noise is seen in upper stratosphere and model underpredicts the temperature
- The origin of the noise is vertical vel time extrapolation in SETTLS
- Solution: use non-extrapolating 1st order scheme for gridpoints with sudden changes in vertical velocity in 2 consecutive steps

Impact of SETTLS time-extrapolation on noisy and smooth data

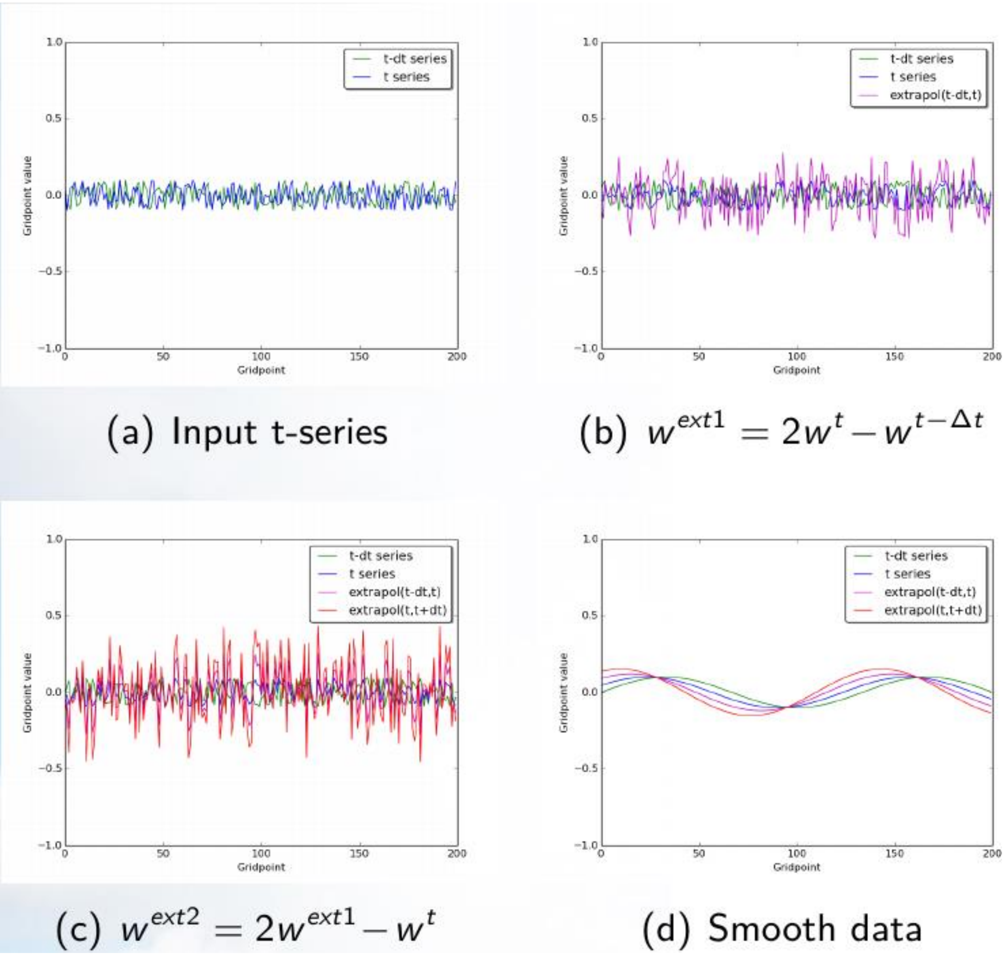

(a) Input t-series

(b) $w^{ext1} = 2w^{t} - w^{t-\Delta t}$

(c) $w^{ext2} = 2w^{ext1} - w^{t}$

(d) Smooth data

Much better representation of Sudden Stratospheric Warming events, due to changes in the Semi-Langrangian scheme (*Diamantakis, 2014*)

NH winter SSWs

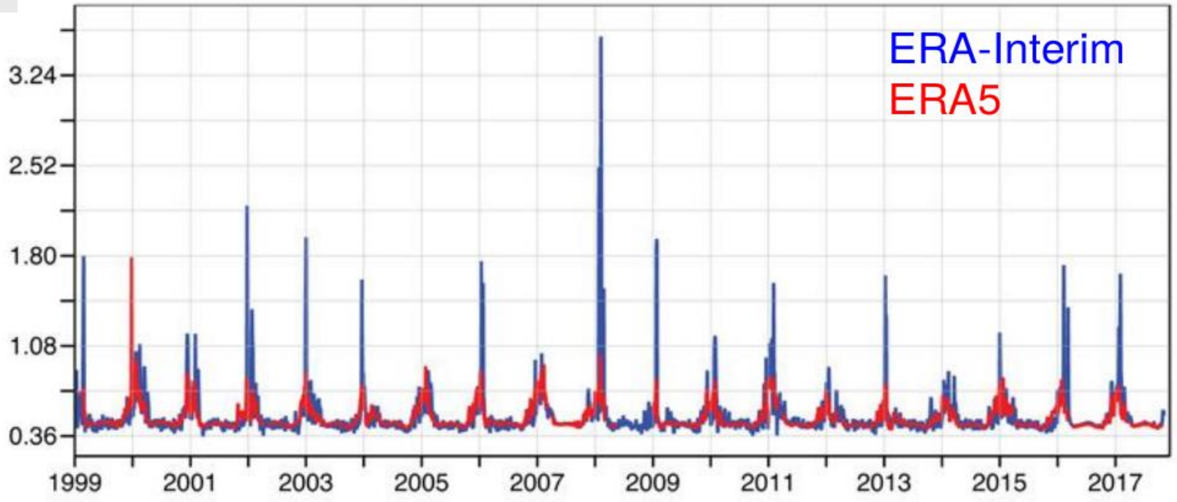

Standard deviation of MW radiances observed vs simulated temperature fields of ERA-Interim (blue) and ERA5 (red) using satellite channel (noaa15) peaking around 5hpa.

T. McNally, A. Simmons

A reference: "Improving ECMWF forecasts of sudden stratospheric warmings", ECMWF newsletter No.141 Autumn 2014

Major SSW January 2013

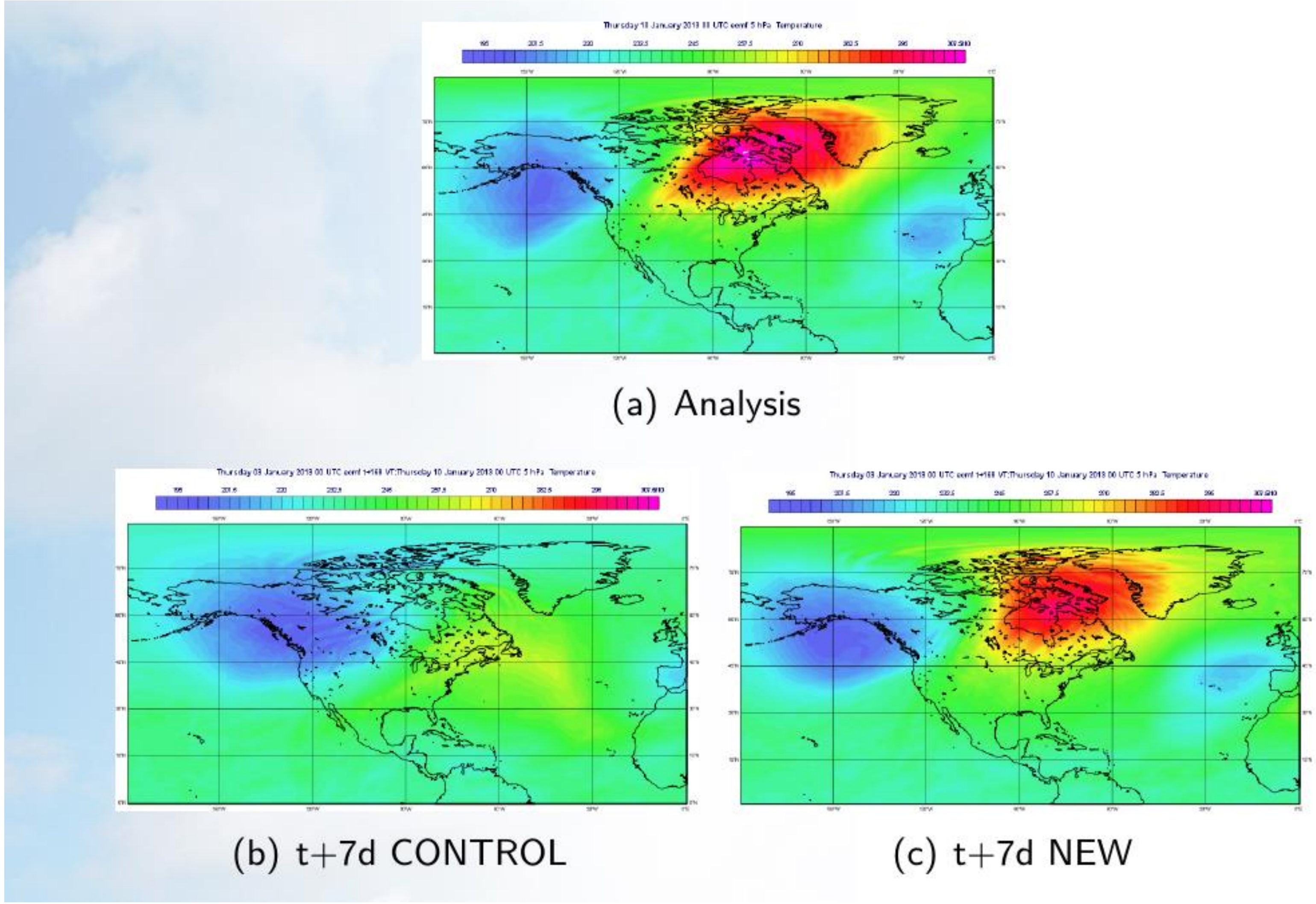

(a) Analysis

(b) t+7d CONTROL

(c) t+7d NEW

Old scheme (CONTROL) versus currently SETTLS scheme

Interpolation in the IFS semi-Lagrangian scheme

After computing the departure points we need to:

- Interpolate the advected field to the DP
- Interpolation must use the gridpoints that lie in the neighbourhood of the DP

ECMWF model uses quasi-monotone quasi-cubic Lagrange interpolation

Cubic Lagrange interpolation: $$\phi(x) = \sum_{i=1}^{4} w_i(x)\phi_i \,, \quad w_i(x) = \frac{\prod_{k \neq i}^{4}(x - x_k)}{\prod_{k \neq i}^{4}(x_i - x_k)}$$

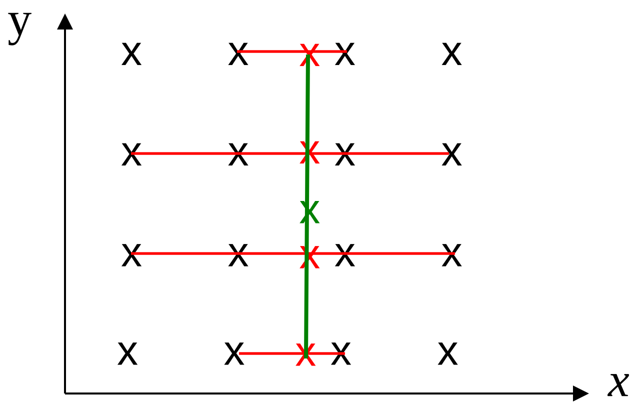

Number of 1D cubic interpolations in 2D: 5 =>3D: 21 (64pt stencil)

To save computations: use *cubic interpolation only for nearest neighbour rows and linear interpolationfor remaining rows. "quasi-cubic interpolation":*

*3*cubic+2*linear interpolations in 2D*

*7*cubic+10*linear in 3D* (32 pt stencil)

Shape-preserving (locally monotonic) interpolation

- Creation of “artificial” maxima / minima

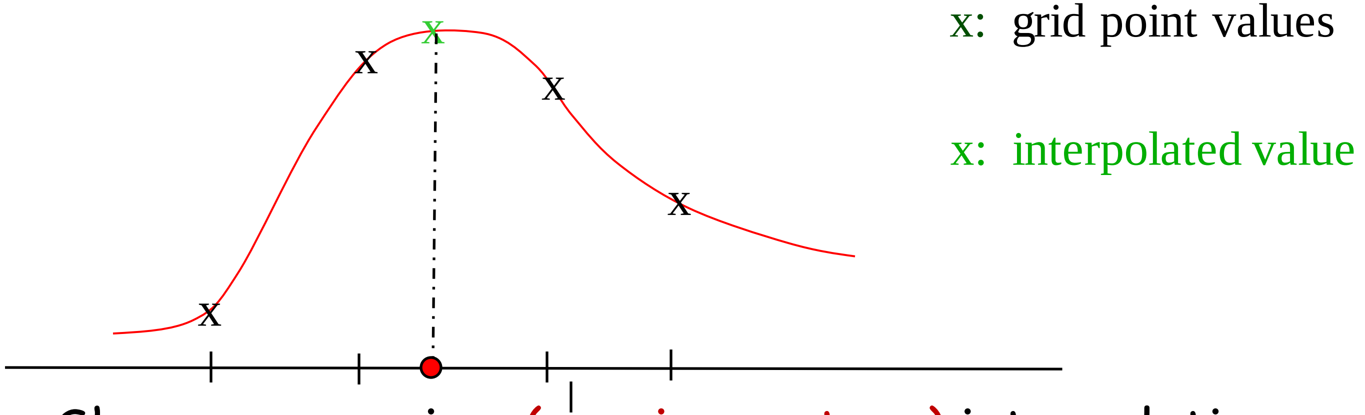

- Shape-preserving (quasi-monotone) interpolation
  - Quasi-monotone cubic interpolation: $\varphi_{qm} = \max(\varphi_{\min}, \min(\varphi_{\max}, \varphi_{cub}))$

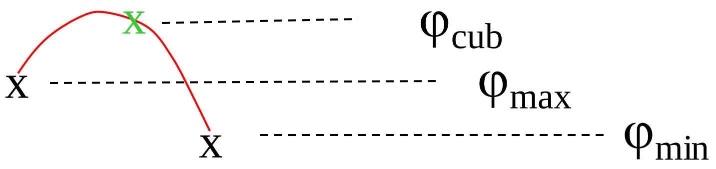

Reducing stratospheric T-bias in 47r1+

Spurious 2Δz noise due to **inadequate vertical-to-horizontal resolution aspect ratio** spuriously **cools** the stratosphere at high horizontal resolution.

Reference: ECMWF newsletter 163, spring 2020 Policthchouk et al

Solutions:

1) increase **vertical resolution** (ENS in 47r3); Expensive!
2) use **quintic** vertical interpolation on T & q in the semi-Lagrangian advection (47r1);
3) **filter 2Δz** noise in T in the semi-Lagrangian advection (SLVF filter by F. Vana, 48r1).

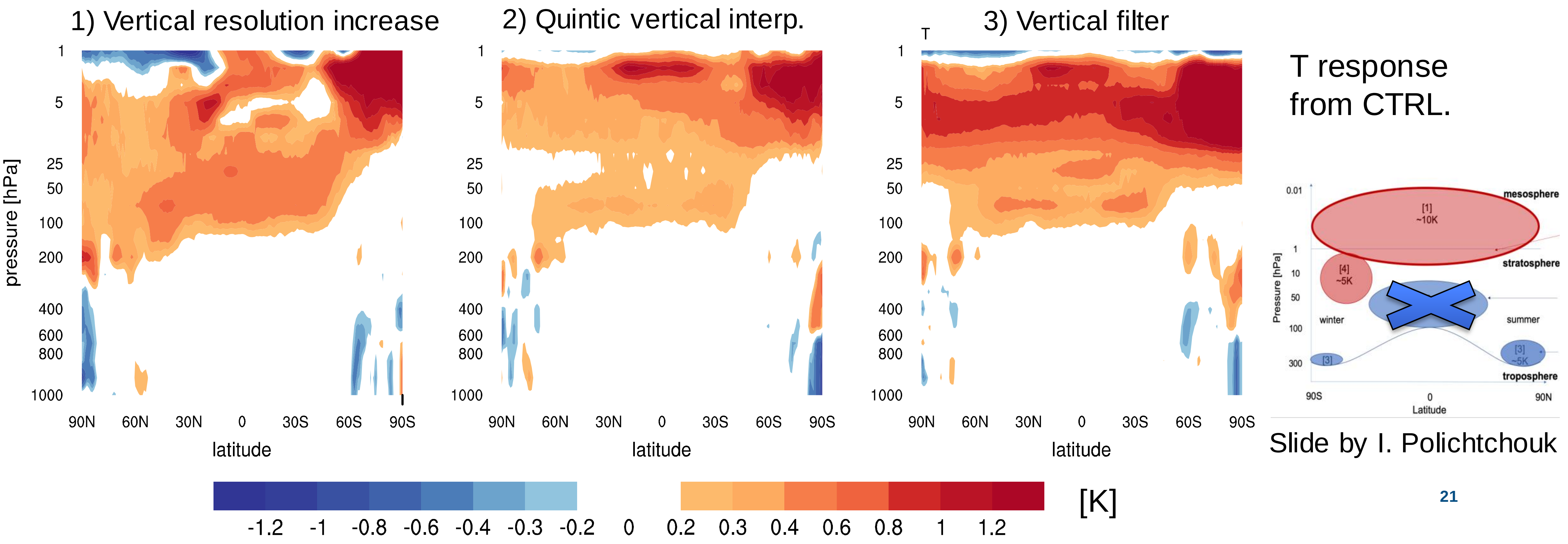

T response from CTRL.

Slide by I. Polichtchouk

Parallel implementation of advection

Interpolation at the DP near the edges of MPI domains requires data from neighbouring domain

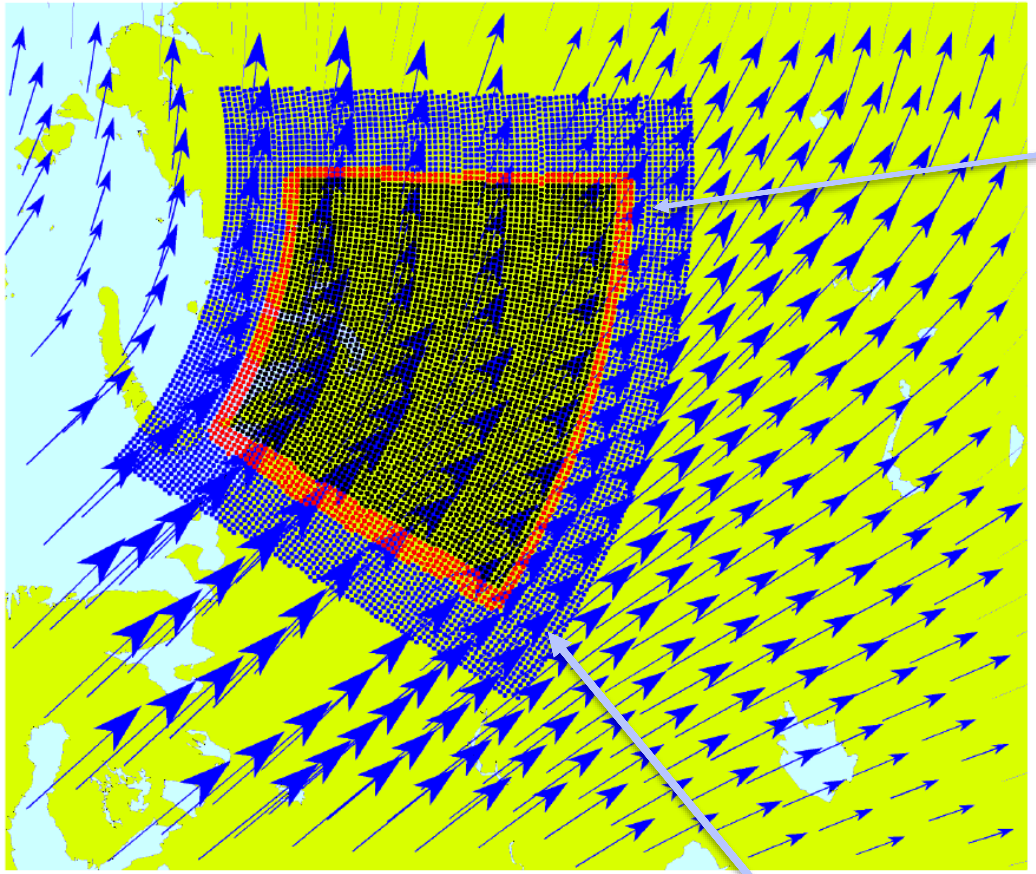

Blue: Halo region

Equal region domain decomposition + MPI and openMP parallel

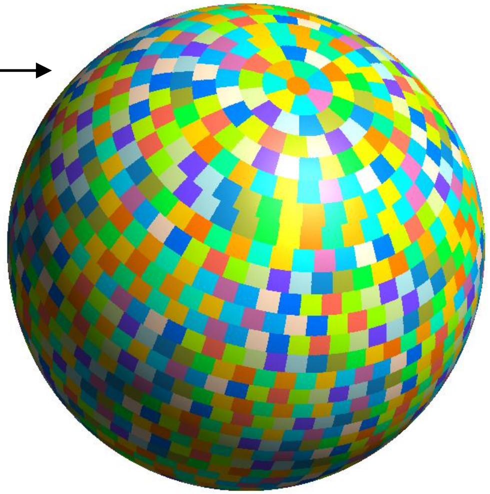

Halo width for MPI assumes a maximum wind speed larger than the ones observed in the atmosphere e.g. 250m/s

Two levels of communication:

- Entire wind halo filled for the DP iterations
- When the DP is known then only a smaller sub-region around the DP needs to be filled
- No need to fetch data from remote processors at the expense of extra memory use

Combining SL with SI to solve prognostic equations

- A nonlinear system of m-prognostic equations must be solved:

$$\frac{DX}{Dt} = M(X), \quad X = (X_1, X_2, \ldots, X_m)$$

e.g. X=(u,v,T,p,q,…)

- Integrate along SL trajectory using 2nd order semi-implicit Crank-Nicolson scheme:

$$X^{t+\Delta t} - X_d^t = \int_t^{t+\Delta t} M(X)dt \Rightarrow X^{t+\Delta t} - X_d^t = \frac{\Delta t}{2}\left(M_d^t + M^{t+\Delta t}\right)$$

Convention: subscript is omitted when variable "sits" at an arrival (grid) point

- An isothermal reference profile is used to linearise terms in M which are responsible for fast wave propagation.

$$\Re = M - L$$

R: nonlinear residual terms; these are changing slowly and can be integrated explicitly

L:"Fast linearized" (e.g. GW) terms. These should be integrated implicitly to permit stable long timesteps

IFS-SISL for NWP prognostic equations

With splitting in fast linear and slow nonlinear residual terms the two-time-level, 2nd order IFS discretization (Temperton et al, QJRMS 2001) becomes:

$$\frac{X^{t+\Delta t} - X_d^t}{\Delta t} = \frac{1}{2}\left(L_d^t + L^{t+\Delta t}\right) + \frac{1}{2}\overbrace{\left(\Re_d^{t+\Delta t/2} + \Re^{t+\Delta t/2}\right)}^{\text{time-extrapolated nonlinear res}}$$

terms interpolated at the DP

The time-extrapolated non-linear residual of the right hand-side is at a trajectory mid-point and can be approximated by the 2nd order SETTLS expansion:

$$\Re_M^{t+\Delta t/2} = \Re_d^t + \frac{\Delta t}{2}\left(\frac{d\Re}{dt}\right)_{AV} \approx \Re_d^t + \frac{\Delta t}{2}\frac{\Re^t - \Re_d^{t-\Delta t}}{\Delta t}$$

Re-arranging terms, yields the familiar SETTLS formula resulting in a 2nd order discretization scheme

$$\frac{X^{t+\Delta t} - X_d^t}{\Delta t} = \frac{1}{2}\left(L_d^t + L^{t+\Delta t}\right) + \Re_M^{t+\Delta t/2}, \qquad \Re_M^{t+\Delta t/2} = \frac{1}{2}\left(\Re^t + \left\{2\Re^t - \Re^{t-\Delta t}\right\}_d\right)$$

all right-hand side terms are given

Helmholtz equation

- Through elimination of variables, previous discretized system is reduced to a single Helmholtz elliptic equation **in terms of horizontal wind divergence**
- Helmholtz equation is solved in spectral space at the end of each timestep
- Constant in time reference profiles ⟹ constant coefficient **Helmholtz equation**
- **Using spherical Harmonics properties Helmholtz equation can be solved very cheaply with a direct diagonal solver (or 5-diagonal when Coriolis terms are implicit)**
    - Having a cheap Helmholtz solver + being able to use large Δt (due to unconditional stability and good dispersion properties of SISL) contributes to high computational efficiency
- Remaining prognostic variables are computed with back substitution

Mass conservation in semi-Lagrangian advection

Mass conservation: important for atmos composition forecasts with long-lived tracers, for long range forecasts, climate and overall, for very high-resolutions

- **In general,** SISL time-stepping does not conserve mass, energy, momentum
- **For tracers**: SL advection cannot conserve mass - interpolation introduces conservation errors
- Mass conservation error depends on the characteristics of the transported variable:
    - Small error for smooth/well mixed with air tracers
    - Large error for localised tracers with large gradients. Monotone limiters result in larger cons errors!
    - Different conservation errors for tracers confined in BL, upper troposphere, stratosphere …

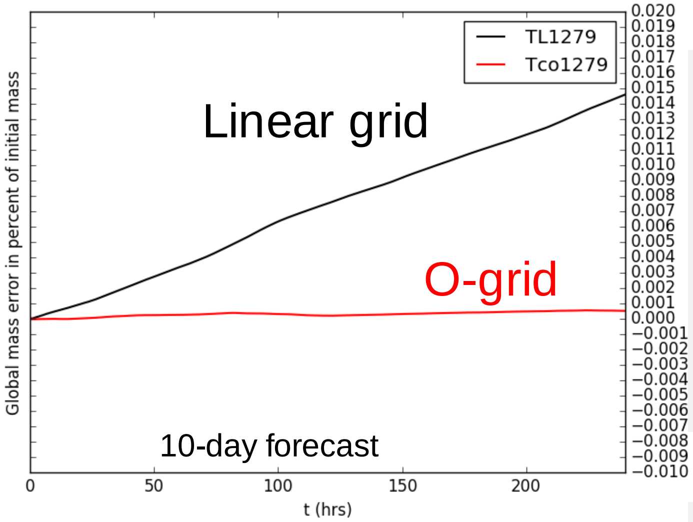

- Total air mass conservation with O-grid is very gooc
(in single-prec there is some degradation and we use mass fixer)

Mass errors as percent of initial mass

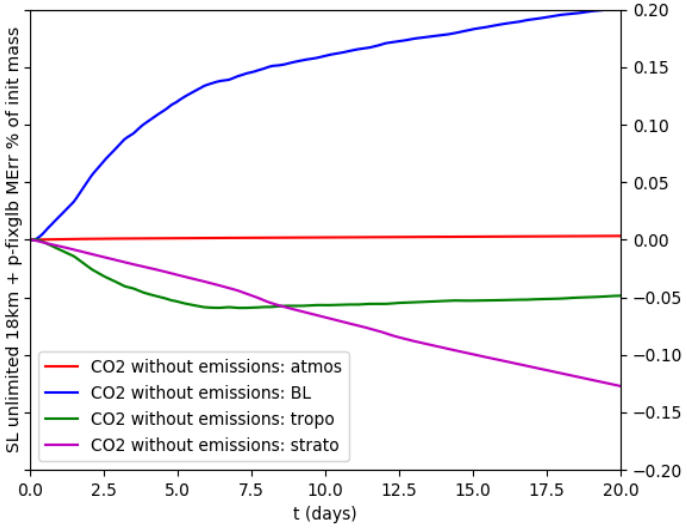

CO_2 glb mass con err:

- Red: CO_2
- Blue: CO_2 tracer confined in the BL
- Green: tracer confined in troposphere above BL
- Purple: tracer confined in stratosphere

Conservation of tracers and numerical order of accuracy

Does the order of accuracy of an interpolation scheme affect mass conservation error?

- For smooth fields conservation error should becoming smaller as the order of accuracy of remapping at the DP (interpolation) increases – it will satisfy at greater accuracy the continuity equation for the tracer
- Indeed, for fields that are relatively smooth and well mixed with air SL advection with high-order interpolation conserves better (co2, ch4, humidity, ozone…)
- *For localized plumes low order could be acceptable or even better*

Mass conservation errors as percent of initial mass

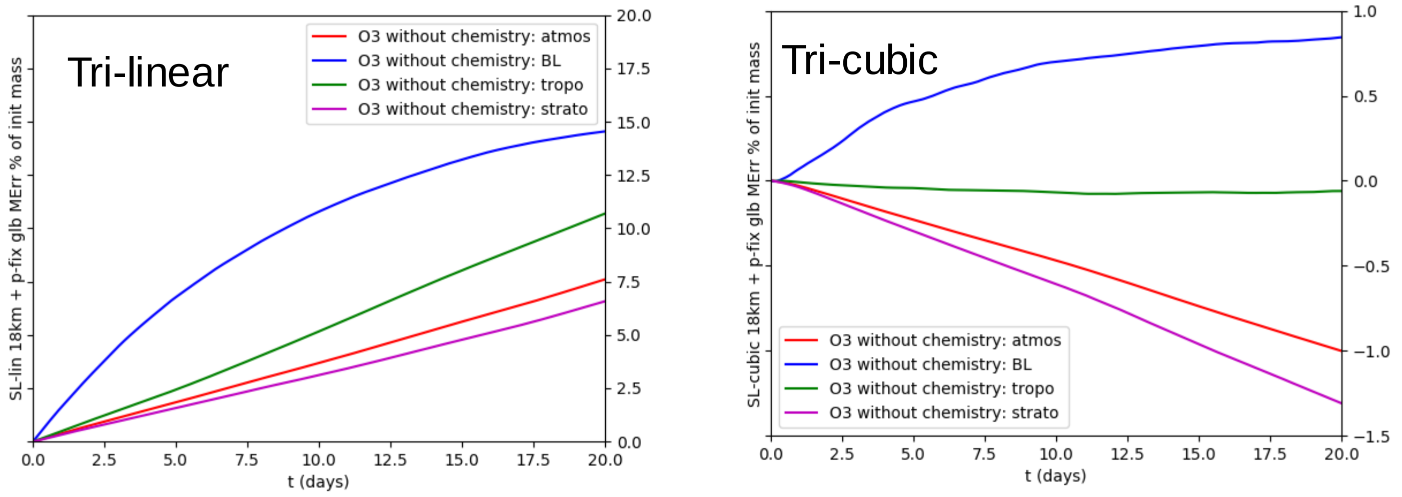

- Big reduction in mass conservation error as interpolation order increases from linear to cubic
- Some further improvement with quintic in the vertical (not shown here)

Tracer mass fixer (active in 48r1)

- **Mass fixers for CAMS tracers have been used for long time**
- **From cycle 48r1 a mass fixer is also applied on water tracers**
- **The tracer mass fixer used is a locally weighted scheme (ECMWF TM 819, 2017 Diamantakis & Agusti-Panareda scheme – inspired from Bermejo & Conde MWR 2002) which gives more skilful tracer concentration predictions apart of correcting their global mass error**

$$\phi_{jk} = \phi_{jk}^{adv} - \lambda w_{jk}, \quad \lambda = \frac{\delta M}{\underbrace{\sum_j A_j \sum_k w_{jk} \frac{\Delta p_{jk}^{adv}}{g}}_{\text{mass integral}}}, \quad \delta M = M\left(\phi_\chi^{adv}\right) - M\left(\phi_\chi^{n}\right)$$

Tracer after advection

M total mass for tracer ϕ

w_{jk} is a weight that depends on the sign of δM, it is proportional to the interpolation truncation error and the mass content of grid-box that corresponds to jk

Correction computed by the mass fixer is the solution of a constrained optimization problem that ensures that its global norm is minimized subject to the constraint that global mass remains constant

Fixing water leakage in IFS

Mass fixer on moist tracers (humidity, clouds): improvement in precipitation scores and overall skill of ENS forecasts

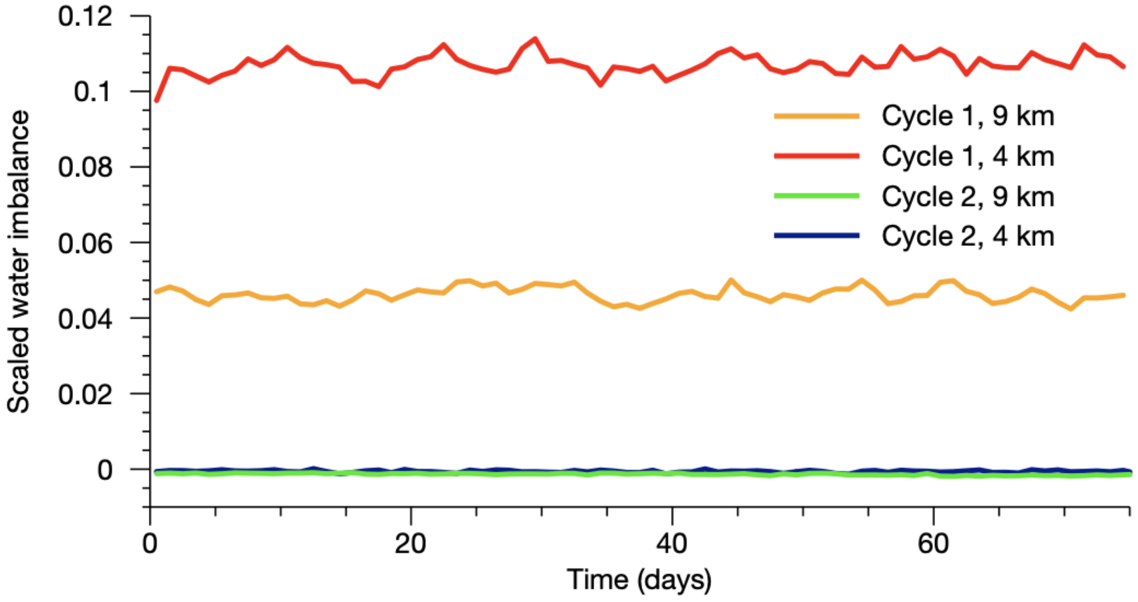

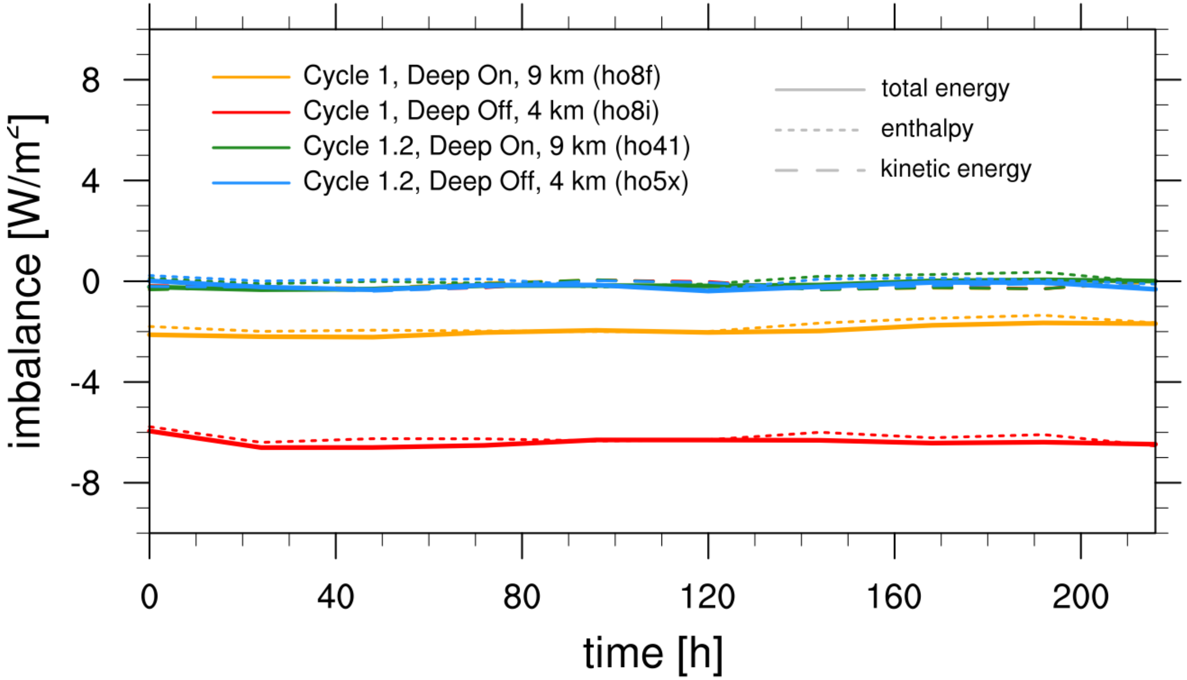

Total water conservation error as a fraction of total precipitation in long integrations

- 10% surplus is reduced to nearly 0% with tracer mass fixer

Total Energy leakage reduction with fixer:
2 W/m2 -> -0.15 (deep conv on)
6 W/m2 -> -0.32 (deep conv off)

Reference: ECMWF newsletter 172, p14

Plots and diagnostics by Tobias Becker from nextGEMS runs

Massfix on GHG: validation against CO2, CH4 observations

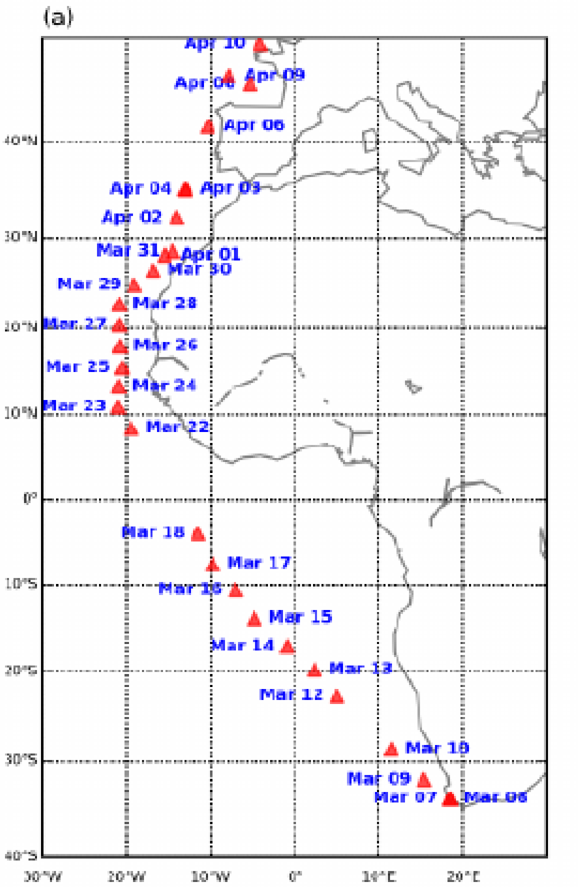

Error without fixer | Error with simple fixer | Error with BC fixer in IFS

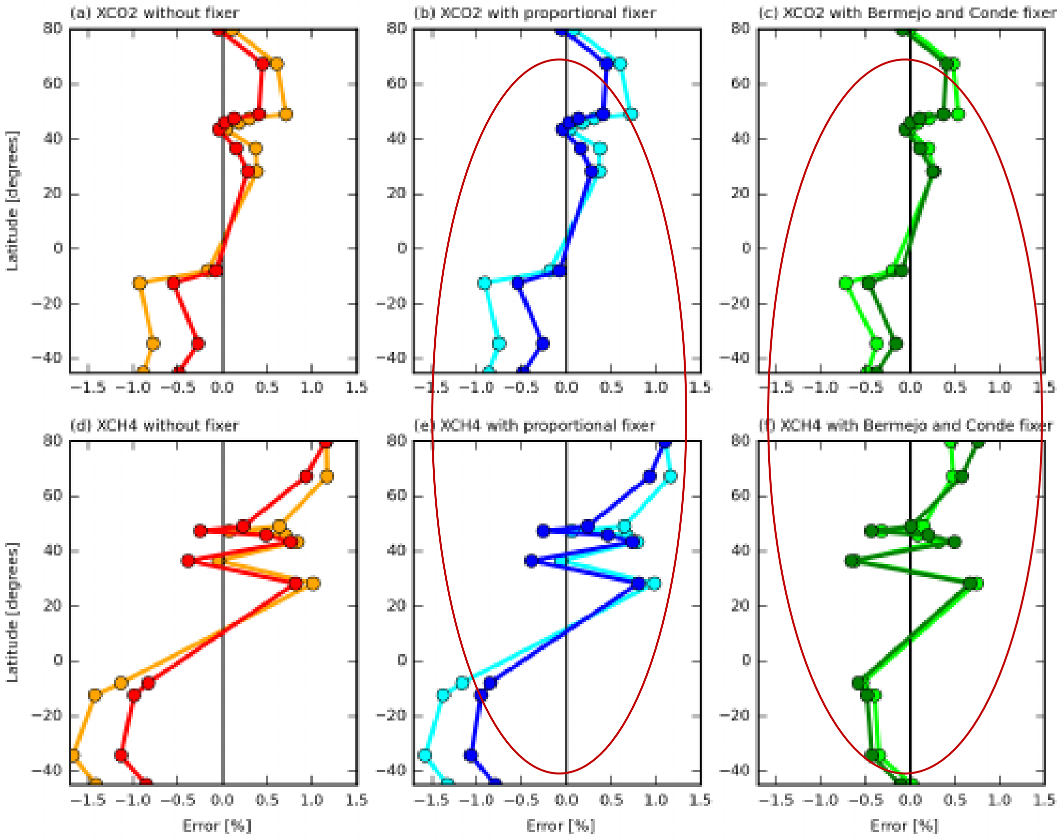

CO2

CH4

Collaboration with CAMS (plots by A. Agusti-Panareda)

Latitudinal monthly mean error (%) distribution at different resolutions for (a-c) XCO2 and (d-f) XCH4 with respect to the observed distribution. Dark colours: low resolution, Light: high resolution. See *GMD 10, 2017, "Improving the inter-hemispheric gradient of total column atmospheric CO2 and CH4 ..."*

Atlas: a library for NWP and Climate modelling

Atlas (Deconinck et al, Computer Phys Coms 2017)

- **Open source code** https://github.com/ecmwf/atlas
- **Flexible data structures**
- **Grid/mesh generation capabilities with parallelization (faster)**
- **Mathematical operators for NWP & climate in HPC environment**
- **C++ or Fortran interface**
- **It supports developments on:**
  - **structured grids**
  - **unstructured hybrid meshes**
- **Parallel algorithms for mesh to mesh interpolation**
- **Accelerator (GPU) capable**

```
grid = atlas_Grid("O1280") ! Create O1280 octahedral Gaussian grid
meshgenerator = atlas_MeshGenerator("structured")
mesh = meshgenerator%generate(grid)   ! Generate mesh from grid
method = atlas_fvm_Method(mesh)       ! Setup finite volume method
nabla  = atlas_Nabla(method)          ! Create FVM nabla operator

call nabla%gradient(scalarfield, gradientfield) ! Compute gradient
```

Cycle 48r1 Atlas capabilities: advection on multiple grids

Demo: O3 advected at 32km grid forced by winds from a 18km grid

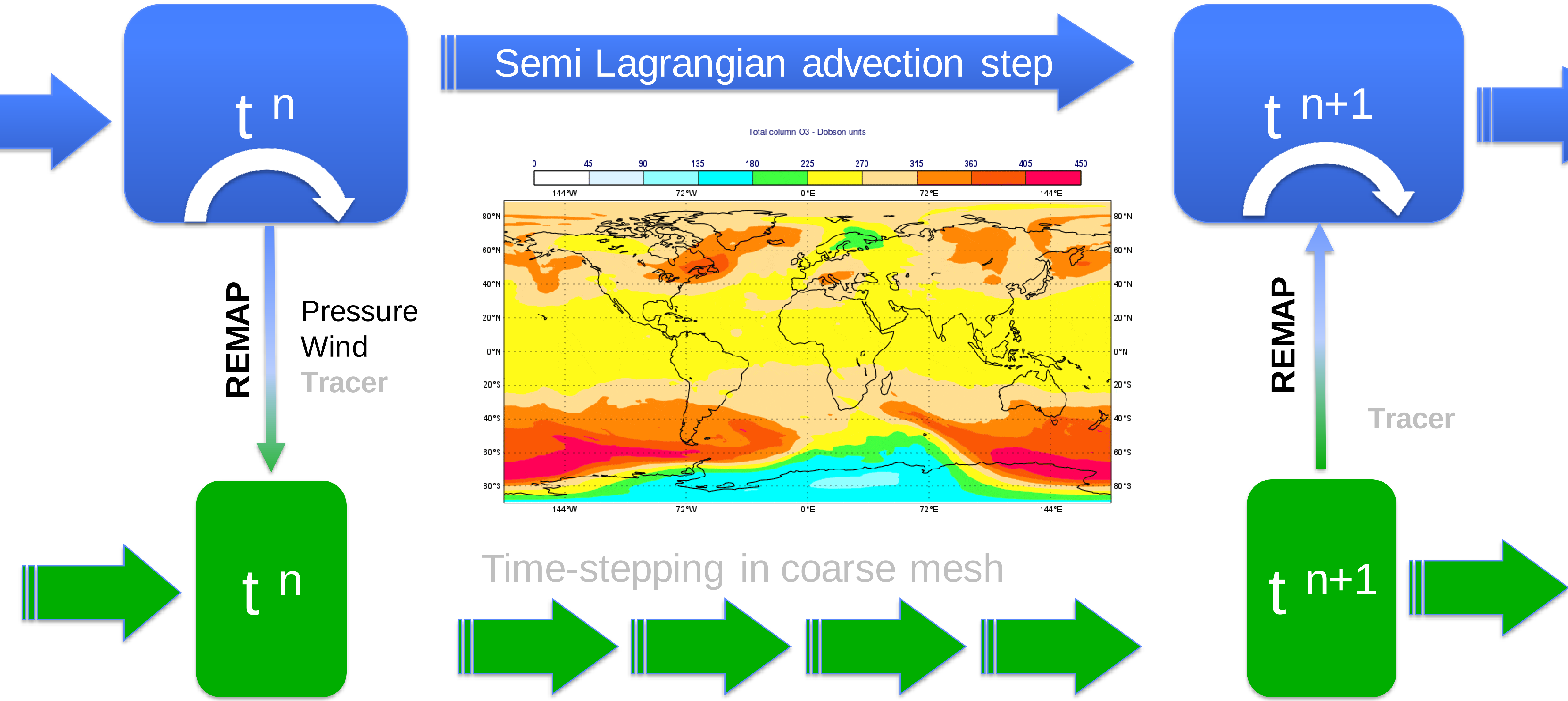

Remapping using linear interpolation (cubic also available)

Thanks to W. Deconinck for ppt schematic

Plug-in MPDATA advection into IFS using Atlas MGRIDS

Nordstream gas leak simulation case study (9km)

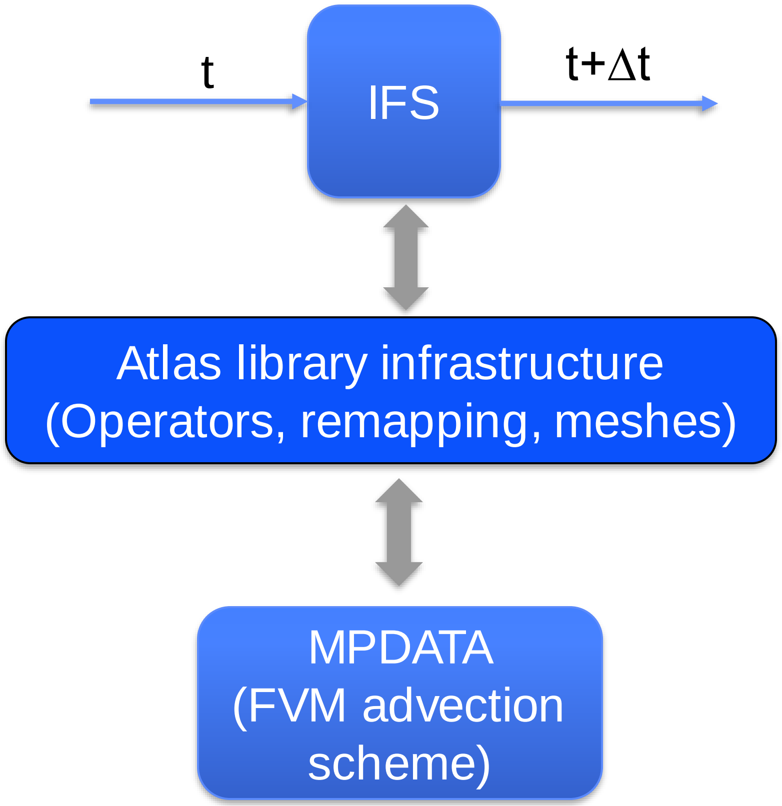

MPDATA simulation using Atlas MGRIDS (driven by IFS winds)

- Same grid Tco1279L137
- Sub-stepping per IFS step due to CFL limit
- Local conservation of MPDATA is advantageous for plumes

SL advection with mass fixer

- Plume results are sensitive to a mass fixer parameter used to compute gridpoint correction for restoring global conservation
- Here, this parameter has been tuned using MPDATA as reference

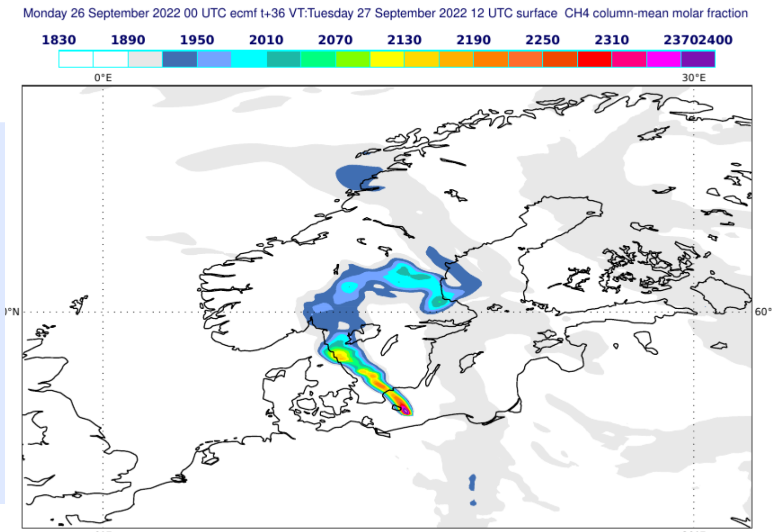

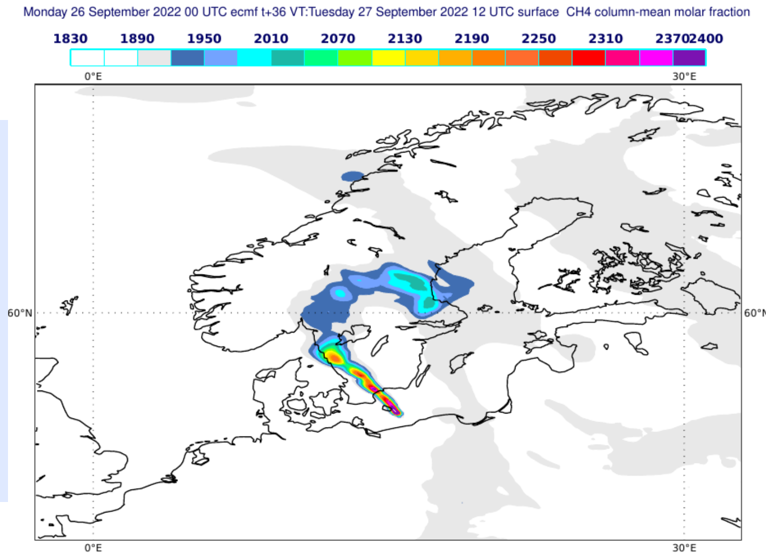

Summary

- IFS relies on an efficient and accurate dynamical core that we constantly improve
- Latest openIFS releases:
  - Improvements in core aspects of the semi-Lagrangian scheme
  - Improvements in tracer mass conservation
  - Fast and accurate with single precision arithmetic
  - Atlas and advection multiple grids capabilities
- Dynamics focus in next years:
  - Improved algorithms for km-scale with a robust and accurate non-hydrostatic (NH) option for evaluation
  - Km-scale IFS H/NH comparisons and analysis of impacts
  - Conservation aspects of tracers (EU funded project *CATRINE=Carbon AtmosphericTracer Research to Improve Numerical Schemes and Evaluation expected to start in 2024 aiming to improve IFS capabilities for future CO2MVS service)*
  - *Development and coupling with physics of a new compact stencil Finite Volume dycore FVM using DSL which is scalable on both CPU and GPU systems well and conserves mass.*

Thank you for your attention!

4.5km resolution global simulation of 10m zonal wind for 1 year

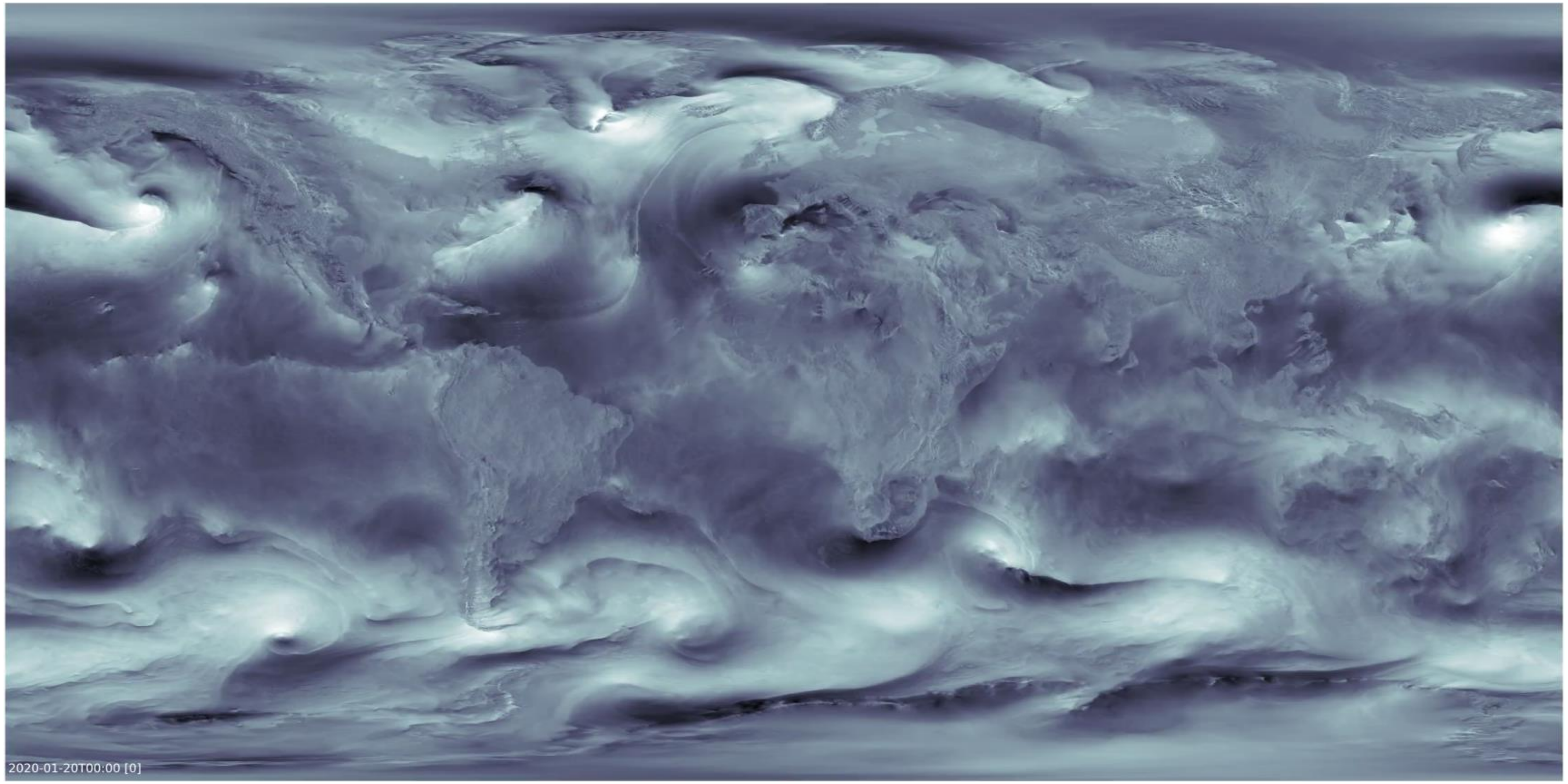

visualisation N. Koldunov (AWI); simulation (T. Rackow, ECMWF)